

White Dwarfs Near Black Holes: A New Paradigm for Type I Supernovae

J. R. Wilson

Lawrence Livermore National Laboratory, Livermore, CA 94550

and

Center for Astrophysics, Department of Physics, University of Notre Dame, Notre Dame, IN 46556

and

G. J. Mathews

Center for Astrophysics, Department of Physics, University of Notre Dame, Notre Dame, IN 46556

ABSTRACT

We present calculations indicating the possibility of a new class of Type I supernovae. In this new paradigm relativistic terms enhance the self gravity of a carbon-oxygen white dwarf as it passes or orbits near a black hole. This relativistic compression can cause the central density to exceed the threshold for pycnonuclear reactions so that a thermonuclear runaway ensues. We consider three possible environments: 1) white dwarfs orbiting a low-mass ($\sim 10 - 20 M_{\odot}$) black hole; 2) white dwarfs encountering a massive ($\sim 1 - 3 \times 10^3 M_{\odot}$) black hole in a dense globular cluster; and 3) white dwarfs passing a supermassive ($\sim 10^6 - 10^9 M_{\odot}$) black hole in a dense galactic core. We estimate the rate at which such events could occur out to a redshift of $z \approx 1$. Event rates are estimated to be significantly less than the rate of normal Type Ia supernovae for all three classes. Nevertheless, such events may be frequent enough to warrant a search for this new class of supernova. We propose several observable signatures which might be used to identify this type of event and speculate that such an event might have produced the observed "mixed-morphology" Sgr A East supernova remnant in the Galactic core.

1. Introduction

Type I supernovae are currently objects of intense interest. The observed luminosity of Type Ia supernovae (SNIa) out to high redshift offers some of the most convincing evidence for the acceleration of the universe due to an unknown dark energy (Garnavich et al 1998; Riess et al. 1998; Perlmutter et al. 1998). The distance redshift relation for the SNIa standard candle is also an important component in the determination of the present cosmic expansion rate (Freedman et al. 2001). As such, it is important to carefully scrutinize any possible variations in the paradigm for SNIa explosions which might occur at large redshift. In this paper we explore one such possible new mechanism for SNIa's.

Type I supernovae are characterized by the absence of hydrogen lines in their spectrum. Type Ia supernovae, in particular, are believed to result from the accretion of material onto the surface of a carbon-oxygen white dwarf. If the accretion rate is sufficiently rapid, mass accumulates until the star approaches the Chandrasekhar limit. As the interior density exceeds the threshold for pycnonuclear reactions, an off-center runaway deflagration/detonation wave of thermal carbon burning ignites under strongly degenerate conditions. Since the degeneracy pressure support of the core is almost independent of temperature, the heating of the core does not cause the star to expand and cool. Therefore, carbon burning rates increase until a thermonuclear explosion eventually engulfs a significant fraction of the star. The key to this paradigm is that the density at some time exceeds the threshold for thermonuclear ignition. For typical Type Ia models the ignition density ranges from $\rho_{ign} \approx 2 - 4 \times 10^9 \text{ g cm}^{-3}$ (at a temperature $T \sim 5 \times 10^8 \text{ K}$) with the lower range of ignition density favored by nucleosynthesis arguments (Iwamoto et al. 1999).

In this paper we propose a new mechanism by which the ignition density of a white dwarf can be achieved. We show that relativistic enhancements of the self gravity of a white dwarf occur whenever the star is accelerating in a background gravitational field. As the velocity with respect to the background field approaches a significant fraction of the speed of light (as will occur near a black hole) these relativistic effects can cause the central density to exceed the threshold for nuclear ignition even for white dwarfs which are well below the Chandrasekhar mass. Alter-

natively, the ignition densities might be achieved by the excitation of tidally-induced resonance/disruption (Khokhlov & Melia 1996; Rathore & Blanford 2000) within the white dwarf, or tidal compression by the Carter-Luminet effect (Carter & Luminet 1982; Laguna, Miller & Aurek 1994). In any of these scenarios, the result is the same, i.e. the ignition of a thermonuclear explosion in a deep gravitational well. The focus of the present work, however, is on the relativistic compression effect (Wilson & Mathews 2000; Wilson 2002).

We note that other authors have modeled hydrodynamic effects which occur as stars encounter a black hole. For example, Fryer et al. (1999) have considered the tidal disruption of a white dwarf near a low mass black hole as a source of gamma-ray bursts. Their simulations were based upon Newtonian hydrodynamics which would not incorporate the general relativistic effect described here. Similarly, Ayal, Livio, and Piran (2000) have simulated the tidal disruption of a normal solar type main-sequence star near a massive ($m \sim 1000 M_{\odot}$) black hole. Extended main sequence stars indeed should tidally disrupt before the relativistic effects described here can induce compression. The effect described here is unique to compact objects such as white dwarfs or neutron stars and is only apparent in a fully relativistic simulation.

We consider three possible environments in which such events might occur. These are: 1) white dwarfs orbiting a low-mass black hole (hereafter LMBHSN); 2) white dwarfs encountering a massive ($M > 1000 M_{\odot}$) black hole in a globular cluster (hereafter MBHSN); and 3) white dwarfs passing a supermassive ($M > 10^6 M_{\odot}$) black hole in a dense galactic core (hereafter SMBHSN). In what follows we utilize general relativistic hydrodynamic numerical simulations described in Sections 2 and 3 to determine the conditions under which the central density can be made to exceed the ignition threshold for these three paradigms. In Section 4 we then make a rough analysis of the event rates at which these various scenarios might occur. We conclude with some discussion as to how such events might be identified observationally.

2. White-Dwarf Compression

It has been noted in studies of colliding (Wilson 2002) and orbiting (Mathews & Wilson 2000) neutron stars that general relativistic effects can overwhelm the stabilizing tidal forces and cause the cen-

tral density of compact objects to increase. This phenomenon was shown (Mathews, Marronetti & Wilson 1998; Mathews & Wilson 2000) to scale with the magnitude of the spatial component of the four velocity of the star relative to the background field for conditions in which there exists no Killing vector by which the three-velocity can be made to vanish.

Here we point out that these conditions are also met for white dwarfs orbiting or passing near a black hole. Thus, a similar scaling of interior density with four velocity should be expected for the case of white dwarfs accelerating under the influence of the gravitation potential of a massive black hole. We show by numerical calculations that the increase of central density is sufficient to induce a thermonuclear runaway and lead to a new class of Type I supernovae. These supernovae are unique in that they would most likely be found in association with a black hole. The case of MBHsNe or SMBHsNe would also be associated with dense globular clusters or galactic cores, respectively. They would also be distinguished from the usual Type Ia event in that they may involve a less massive white dwarf and a rapid ignition/detonation in their centers.

2.1. The Model

We analyze the induced compression in the context of a general relativistic treatment of the hydrodynamic and field evolution of a white dwarf in the vicinity of a black hole. Although an orbiting system is inherently nonaxisymmetric, the essential features of this system can be modeled (with slight modifications) while imposing axisymmetry. The implementation of axisymmetry does not lead to significant inaccuracies, but it allows us to rapidly explore a broad range of parameter space for white-dwarf plus black-hole systems as follows.

An exact axisymmetric general relativistic hydrodynamic model has been previously developed by Wilson (1979; 2002) (see also Hawley, Smarr & Wilson 1984) to describe the head-on collision of two neutron stars. Here we have modified this model to treat the essential features of a white-dwarf plus black-hole system.

We start with the ADM formalism (Arnowitt, Deser & Misner 1962) whereby, the metric is split into space-like and time-like components

$$ds^2 = -(\alpha^2 - \beta_i \beta^i) dt^2 + 2\beta_i dx^i dt + \gamma_{ij} dx^i dx^j \quad , \quad (1)$$

where α is the lapse function, β^i is the shift vector,

and γ_{ij} is the metric for the three-space (we use geometrized units. $G = c = 1$). For the present purposes, we are concerned with either quasi-stationary orbits or passing orbits near the point of closest approach. In either case, the β^r and β^z metric components are very small for the systems of interest here and can be neglected in what follows. In a full nonaxisymmetric treatment, the dominant contribution to the shift vector will be from nonaxisymmetric motion about the rotation axis of the orbit plane. Nevertheless, an axisymmetric model can still be maintained by modified hydrodynamic equations as described below.

In essence there are two effects of orbital motion on the shift vector: In a comoving gauge (Wilson & Mathews 2003) the dominant contribution is from an overall rotation of the coordinates. The explicit inclusion of this term naturally generates the appropriate centrifugal and Coriolis forces associated with a rotating coordinate system. There is also a small Lense-Thirring frame-drag correction (Wilson, Mathews & Marronetti 1996) for the relativistic orbit precession. The frame-drag component can be deduced from an equation of the form, $\nabla^2 \beta_{drag} \approx 16\pi\alpha\phi^4 W \rho_{WD} U$ (Wilson & Mathews 2003). For the systems of interest here, the source term is small so that frame-drag is only a small correction to the orbital motion. This is consistent with numerical results for neutron-star binaries near their last stable orbit (Mathews & Wilson 2000). Hence, for our purposes the frame-drag can be neglected.

The coordinate rotation term can be eliminated by choosing an instantaneously nonrotating coordinate system at the orbit periape and adding effective centripetal force terms to the equations of motion as described below.

Thus, for this application we adopt a quasi-Eulerian ($\beta_i = 0$) gauge (Wilson & Mathews 2003). We further adopt a conformally flat metric whereby $\gamma_{ij} = \phi^4 \delta_{ij}$. This has been shown (Cook et al. 1993; Mathews & Wilson 2000; Wilson 2002) to be sufficiently accurate for our purpose.

Thus, in cylindrical coordinates we write an effective metric ,

$$ds^2 = -\alpha dt^2 + \phi^4 [dr^2 + dz^2 + r^2 d\theta^2] \quad , \quad (2)$$

where in what follows we take the z coordinate to be the distance along the line of centers between the black hole and the white dwarf. The r coordinate is the radius perpendicular to the z axis. This metric

leads (Wilson, Mathews & Marronetti 1996; Wilson 2002; Wilson & Mathews 2003) to simple Poisson-like elliptic constraint equations which can be solved to find the the conformal factor and lapse function.

$$\begin{aligned} \nabla^2 \phi &= -2\pi\phi^5 \left[DW + E \left(\Gamma W - \frac{\Gamma - 1}{W} \right) \right. \\ &\quad \left. + \frac{1}{16\pi} K_{ij} K^{ij} \right] . \end{aligned} \quad (3)$$

$$\begin{aligned} \nabla^2(\alpha\phi) &= 2\pi\alpha\phi^5 \\ &\times \left[\frac{D(3W^2 - 2) + E[3\Gamma(W^2 + 1) - 5]}{W} \right. \\ &\quad \left. + \frac{7}{16\pi} K_{ij} K^{ij} \right] . \end{aligned} \quad (4)$$

where the source term includes Lorentz contracted state variables, $D = \rho W$, $E = \epsilon\rho W$, with ρ the local proper mass density, ϵ the internal energy per unit mass, and W a Lorentz-like factor, $W = \sqrt{1 + U^i U_i}$, where U^i denotes spatial components of the four velocity.

The quantity $\Gamma \equiv 1 + P/\epsilon\rho$ is an equation of state index. We use a standard white dwarf equation of state (e.g. Salpeter 1961; Hamada & Johnson 1961) to specify ϵ and/or Γ as a function of density. For simplicity we only retain the dominant degenerate electron part.

In equations (3) and (4) the extrinsic curvature $K_{ij} K^{ij}$ terms result (Wilson & Mathews 2003) from derivatives of the relativistic frame drag contained in the β^i . In close neutron-star binary systems it has been shown (Mathews & Wilson 2000) that this term contributes insignificantly to the metric source terms, ($\int dV K_{ij} K^{ij} / 8\pi \sim 10^{-5} M_{Grav}$). In what follows these extrinsic curvature terms can therefore be neglected. Including these terms would only slightly enhance the compression effect described below.

2.2. Axisymmetric Hydrodynamics

To model a white dwarf near a black hole, a centrifugal term is added to the axisymmetric momentum equations to keep the stars apart. Thus, the hydrodynamic equations are slightly modified from those presented in (Wilson 2002; Wilson & Mathews 2003) The momentum equation becomes,

$$\frac{\partial S_i}{\partial t} + 6S_i \frac{\partial \ln \phi}{\partial t} + \frac{1}{\phi^6} \frac{\partial}{\partial x^j} \left(\phi^6 S_i V^j \right) + \alpha \frac{\partial P}{\partial x^i}$$

$$\begin{aligned} &+ \sigma\alpha \left[(1 + U^2) \frac{\partial \ln \alpha}{\partial x^i} - 2U^2 \frac{\partial \ln \phi}{\partial x^i} \right] \\ &- \sigma \frac{U^2}{z} \delta_{iz} = 0 , \end{aligned} \quad (5)$$

where $\sigma \equiv D + \Gamma E$, and the covariant coordinate momentum density is $S_i = \sigma U_i$, and $U^2 \equiv U_i U^i$.

The last term in Eq. (5) is a centrifugal acceleration. It accounts for the conserved motion along an unspecified third coordinate perpendicular to z . Obviously, setting this term to zero recovers the simple head on collision. If this term is sufficiently large, it can stabilize the stars in orbit, or it can limit motion along z to a distance of closest approach.

It is to be noted that this component must be included in the $U_i U^i$ summations above and in the metric fields. For example, at closest approach, $U^2 = U_\perp U^\perp$. Thus, the inclusion of this term increases the source terms [cf. Eqs. (3) and (4)] for the solution of the metric fields.

The remaining hydrodynamic equations assume their usual form. The continuity equation is,

$$\frac{\partial D}{\partial t} + 6D \frac{\partial \ln \phi}{\partial t} + \frac{1}{\phi^6} \frac{\partial}{\partial x^j} (\phi^6 D V^j) = 0 . \quad (6)$$

The equation of internal energy evolution is,

$$\begin{aligned} \frac{\partial E}{\partial t} &+ 6\Gamma E \frac{\partial \ln \phi}{\partial t} + \frac{1}{\phi^6} \frac{\partial}{\partial x^j} (\phi^6 E V^j) \\ &+ P \left[\frac{\partial W}{\partial t} + \frac{1}{\phi^6} \frac{\partial}{\partial x^j} (\phi^6 W V^j) \right] = 0 , \end{aligned} \quad (7)$$

2.3. Enhanced Self Gravity

The term with $\sigma\alpha\partial \ln \alpha/\partial x^i$ in Eq. (5) is the relativistic analog of the Newtonian gravitational force. The general relativistic condition of hydrostatic equilibrium for each star can be inferred by taking the time-stationary limit of the momentum equation (5), and transforming to instantaneously comoving three space coordinates with a grid velocity $x_g^i = x^i - V_g^j dt$ such that the three velocity $V^j - V_g^j = 0$. This gives

$$\frac{\partial P}{\partial x^i} = -\sigma \left(\frac{\partial \ln \alpha}{\partial x^i} + U^2 \left[\frac{\partial \ln \alpha}{\partial x^i} - 2 \frac{\partial \ln \phi}{\partial x^i} \right] \right) . \quad (8)$$

Note, that in the weak-field limit, $\phi^2 \approx \alpha^{-1}$ which reduces Eq. (8) to

$$\frac{\partial P}{\partial x^i} \approx -\sigma \frac{\partial \ln \alpha}{\partial x^i} \left(1 + 2U^2 \right) , \quad (9)$$

from which it is manifestly apparent that the terms in the square brackets of Eq. (8) do not cancel. The enhanced self gravity derives from the additional U^2 dependent terms of Eqs. (8) and (9).

3. Model Calculations

As noted above, we consider several possibilities in this study. One is a white dwarf in a bound orbit around a low-mass black hole. This situation could result, for example, from the evolution of a binary in which one member was a massive progenitor which formed a black hole. Alternatively, a white dwarf might be captured by a black hole through three-body interactions in a dense cluster. In either case, the white dwarf orbit would decay by gravitational radiation until it approaches high orbital velocity. Another possibility is that of a white dwarf randomly passing a massive $\gtrsim 1000 M_\odot$ black hole in a dense globular cluster or galactic core.

To start each calculation an initial distribution of density and internal energy is taken (e.g. a white dwarf in hydrostatic equilibrium) and with initial velocities corresponding to either nonradial infall from infinity, or of an amount required to stabilize the orbit, i.e. an angular momentum is chosen to present a centrifugal barrier. In the case of a simple bound circular orbit, this term was simply adjusted to keep the white dwarf at a fixed distance from the black hole. For the case of passing orbits, this term was chosen to produce a particular distance of closest approach. The stars were then evolved and the central density monitored until the white dwarf was either tidally disrupted, attained the critical density for thermonuclear burn, or passed the distance of closest approach.

For our purposes, a thermonuclear runaway is conservatively expected to initiate once the density exceeds $3 \times 10^9 \text{ g cm}^{-3}$. Table 1 summarizes key properties of white dwarfs of various mass in bound circular orbits around low-mass black holes. Tables 2 and 3 summarize some calculations of passing orbits of massive and supermassive black holes, respectively, at the points of closest approach. For illustration, column 3 in these tables gives ρ_c^∞ the central density for isolated white dwarfs of the indicated mass.

Most of these table entries have been selected because they represent systems which have just achieved the ignition density in their centers at the distance of closest approach. The two entries of a $1.2 M_\odot$ white dwarf orbiting a low mass black hole, however,

are just below our adopted ignition density. All of the stars in Table 1 have large tidal distortion even though their central density is quite high.

Figures 1 to 3 illustrate the competition between tidal distortion and relativistic compression. These figures are for a typical $0.6 M_\odot$ white dwarf passing near various massive black holes. Note, that the radius of an isolated $0.6 M_\odot$ white dwarf is $\sim 9000 \text{ km}$. Hence, these stars are significantly compressed. The black hole resides at $\sim 10^4 \text{ km}$ below these figures as noted in the captions. All three cases have been chosen because the white dwarf just achieves the ignition threshold in its center near the point of closest approach to the black hole. These therefore represent the maximum impact parameter for which explosion can occur.

Figure 1 is for a white dwarf near a $1000 M_\odot$ black hole. In this case, the white dwarf is substantially tidally distorted. Nevertheless it has compressed (by more than a factor of 1000 in density and a factor of 10 in radius) so that the center reaches the ignition threshold. Figure 2 is for a $1500 M_\odot$ black hole. It shows less tidal distortion since it reaches the central ignition density farther from the star. Similarly, Figure 3 for a white dwarf even farther from a $3000 M_\odot$ black hole exhibits almost no tidal distortion at all. These figures clearly illustrate that for such systems, the tidal forces (which tend to decrease the central density) are not strong enough to prevent an increase in central density as the white dwarf approaches the black hole.

From these simulations the following conclusions can be made regarding this paradigm:

- Substantial increases in central density can occur as a star passes close to a black hole. For example, the central density of a $0.6 M_\odot$ white dwarf in isolation is $3.2 \times 10^6 \text{ g cm}^{-3}$. This density is increased by nearly a factor of 10^3 when passing a massive black hole.
- The ignition density can be achieved for smaller velocities for white dwarfs that are closer to the Chandrasekhar mass.
- For low-mass black holes, pycnonuclear ignition requires the orbit to be relatively close ($\sim \text{few} \times 10^3 \text{ km}$), i.e. comparable to the radius of the white dwarf. Also, the white dwarf must be in the high end of the observed mass distribution, $M_{WD} > 1.2 M_\odot$. However, For a black

TABLE 1
WHITE DWARFS ORBITING A BLACK HOLE

M_{WD} (M_{\odot})	M_{BH} (M_{\odot})	ρ_c^{∞} (10^9 g cm $^{-3}$)	ρ_c (10^9 g cm $^{-3}$)	z_{min} (km)	U^2
1.20	10	0.12	1.2	4.82×10^3	0.0031
1.20	20	0.12	1.6	6.52×10^3	0.0045
1.30	10	0.37	2.9	4.21×10^3	0.0035
1.30	20	0.37	3.0	5.77×10^3	0.0051

TABLE 2
WHITE DWARFS PASSING A MASSIVE BLACK HOLE

M_{WD} (M_{\odot})	M_{BH} (M_{\odot})	ρ_c^{∞} (10^9 g cm $^{-3}$)	ρ_c (10^9 g cm $^{-3}$)	z_{min} (km)	U^2
0.60	1000	0.0032	3.4	0.120×10^5	0.248
0.60	1500	0.0032	3.2	0.193×10^5	0.231
0.60	3000	0.0032	3.9	0.393×10^5	0.226
0.80	3000	0.0091	3.6	0.706×10^5	0.126
1.00	3000	0.029	3.1	1.24×10^5	0.0715
1.20	3000	0.12	3.1	2.81×10^5	0.0316
1.30	3000	0.37	3.2	5.50×10^5	0.0160
1.40	3000	1.9	3.2	33.0×10^5	0.0027

TABLE 3
WHITE DWARFS PASSING A SUPERMASSIVE BLACK HOLE

M_{WD} (M_{\odot})	M_{BH} (M_{\odot})	ρ_c^{∞} (10^9 g cm $^{-3}$)	ρ_c (10^9 g cm $^{-3}$)	z_{min} (km)	U^2
0.60	10^9	0.0032	3.06	1.5×10^{10}	0.191
0.70	10^9	0.0056	3.29	2.0×10^{10}	0.151
0.80	10^9	0.0091	3.05	2.5×10^{10}	0.118
0.90	10^9	0.010	2.95	3.3×10^{10}	0.0905
1.00	10^9	0.029	3.13	4.3×10^{10}	0.0686

hole of $m_{BH} \geq 1000 M_{\odot}$ sufficient compression can occur even for a $0.6 M_{\odot}$ white dwarf, and ignition can occur much further from the black hole where tidal effects are minimal (cf. Fig. 3).

Hence, we conclude that the most likely environment for this effect is in a dense galactic core or globular cluster in which there is a good chance that a white dwarf can pass relatively close to a massive or supermassive black hole.

4. Event Rates

4.1. Normal Type Ia Supernovae

It is important to have an estimation of the rates of such new events relative to those of normal SNIa's. The observable event rate for normal SNIa explosions out to a redshift of $z \approx 1$ is rather significant

$$\dot{N}_{SNI} = N_{gal} \dot{R}_{Ia} \approx 10^9 \times 10^{-2} \approx 10^7 \text{ yr}^{-1} \quad , \quad (10)$$

where N_{gal} is the number of galaxies out to $z \approx 1$, and R_{Ia} is the average rate per galaxy at which carbon-oxygen white dwarfs accrete enough material to exceed the critical interior density for the ignition of an explosion. This rate is observed to be about 1 per century per galaxy (Kobayashi et al. 2000). It is instructive, however, to review how one estimates this rate theoretically:

If we adopt the current view that Type Ia supernovae arise from the binary accretion of material onto a white dwarf. There are two scenarios which have been debated in the literature (Nomoto et al. 1994; Kobayashi et al 2000). The most widely adopted from a theoretical modeling point of view (and the one that will be adopted here) is that of a single degenerate white dwarf which accretes hydrogen via mass transfer from a normal red giant or main sequence companion. If the mass transfer is sufficiently rapid, the interior density rises to the ignition density before material can be ejected via normal nova eruptions. A second possibility (Iben & Tutukov 1984; 1985) is that of a doubly degenerate carbon-oxygen white-dwarf binary. The eventual merger of the two white dwarfs leads to a single system of order the Chandrasekhar mass which can ignite and explode.

The relative rates of either of these paradigms can be deduced from the relative probability of having a close interacting binary. For this we utilize a slightly modified version (Mathews, Bazan & Cowan 1992)

of an expression first proposed by Greggio & Renzini (1983).

$$R_{Ia}(t) = \int_{M_l}^{M_h} dM_B \phi(M_B) \int_{q_l}^{q_h} dq f(q) \times \int_{a_l(t, M_B, q)}^{a_h(t-\tau, M_B, q)} da P(a) \psi(t - \tau) \quad , \quad (11)$$

where $\phi(M_B)$ is the initial mass function (IMF) for a binary of total mass, M_B , $f(q)$ is the distribution function for the ratio of the secondary to primary mass, $q = m_2/m_1$, $P(a)$ is the distribution of initial separations, a , and $\psi(t - \tau)$ is the star formation rate corrected for the evolutionary time τ for the secondary star to evolve to a white dwarf and for the binary to evolve to a supernova. As in (Mathews, Bazan & Cowan 1992) we take $f(q) \propto q^x$ with $x < 2$, since distributions with exponents ≥ 2 give incorrect ratios of single lined to double lined spectroscopic binary systems (Kraicheva *et al.* 1979). This favors mass-symmetric systems. The initial separation distribution is taken by similar arguments (Tutukov & Yungelson 1979) to be $P(a) \propto a^{-1}$, which favors close systems.

The upper and lower limits to the mass integral are simply the largest and smallest total binary mass, respectively, allowed by the scenario and evolutionary time scale. For a single degenerate white dwarf SNIa, one typically has, $1 \leq m_2 \leq 3 M_{\odot}$ and $3 \leq m_1 \leq 8 M_{\odot}$ as the carbon-oxygen white dwarf progenitor. This implies, $M_l = 4$, $M_h = 11$ and $q_l = 1/8$, $q_h = 1$. The limits on the separation distance are determined by the presumed scenario for Type Ia supernovae as discussed above. For our purposes, the lower limit $a_l \sim 10$ AU is determined (Mathews et al. 1992) by the requirement that the stars not be too close during the common-envelope asymptotic-giant-branch phase (Iben & Tutukov 1984; 1985) of the white dwarf progenitor to prevent the formation of a CO white dwarf.

4.2. White Dwarfs Orbiting a Black Hole

One might think that a white dwarf orbiting a common low-mass black hole could be the most likely candidate for this event. After all, a number of candidate binary systems have been identified (Cowley 1992) which probably contain a black holes as one member. Indeed, mass transfer from a close companion star is the primary means to identify a black hole candidate. Hence, it seems quite likely that a number of close binary systems exist in which the higher-mass

progenitor star has evolved to a black hole while the lower-mass member is now a white dwarf. In this case, the inspiraling of the white-dwarf companion is an inevitable outcome and the possibility of a compression-induced explosion needs to be considered. Here, we estimate the rate of such events relative to normal SNIa events. We find that this is a possible, though rare, phenomenon.

The relative rate of exploding white-dwarf, black-hole binaries compared to that of normal Type I supernovae can be deduced from Eq. (11). Ignoring the logarithmic dependence on relative separation, and assuming instantaneous recycling along with a Salpeter IMF, the ratio of rates becomes:

$$\frac{R_{LMBHSN}}{R_{SN1a}} \approx \frac{[M_l^{-1.3} - M_h^{-1.3}]_{LMBHSN}}{[M_l^{-1.3} - M_h^{-1.3}]_{SN1a}} \times \frac{[q_{max}^{x+1} - q_{min}^{x+1}]_{LMBHSN}}{[q_{max}^{x+1} - q_{min}^{x+1}]_{SN1a}}. \quad (12)$$

Adopting the parameters above for the carbon-oxygen white dwarf progenitor, and progenitor masses for a low-mass black hole in the range of $20 \leq m_1 \leq 60$, we have $M_l = 23$, $M_h = 68$, $q_{min} = 0.04$, and $q_{max} = 0.40$ for the LMBHSN scenario. Setting $x = 1$ then implies a most optimistic rate of

$$\frac{R_{LMBHSN}}{R_{SN1a}} \approx 10^{-3}. \quad (13)$$

Requiring that the white dwarf have a mass $M_{WD} > 1.2 M_\odot$ and that the progenitor star produce a black hole with $M_{BH} \geq 20 M_\odot$ (as indicated in Table 1) will decrease this rate by at least another order of magnitude. Hence, we conclude that this type of supernova is probably much less frequent than normal Type Ia supernovae. The main reason is the simple fact that the high-mass progenitors of a black hole are more rare than the low-mass progenitors which can produce SNIa's. Also, the required massive white dwarfs are rare, and the required binary systems with a high mass asymmetry are less common.

5. White Dwarfs Passing a BH

The other plausible candidate environments for the explosion scenario considered here are those of white dwarfs on passing orbits near a massive ($m_{BH} \sim 10^3 M_\odot$) black hole in the center of a globular cluster or a supermassive ($m_{BH} \sim 10^6 - 10^9 M_\odot$) black hole in a dense galactic core. We show here that is possible for event rate in these environments to be greater

than the event rate due to low-mass black-hole/white-dwarf binaries. Supermassive black holes, for example, appear to be present in every galaxy. They also tend to be found in high density stellar environments in which a large encounter rate is possible.

5.1. Massive Black Hole in Globular Clusters

At the present time there is no firm observational evidence for massive black holes in globular clusters (GCs) even though much effort has been expended searching for them. Although there have been recent claims (e.g. Gebhardt, Rich & Ho 2002; van der Marel et al. 2002) for their detection, it has since been demonstrated (cf. Baumgardt et al. 2003; Ferraro et al. 2003; McNamara 2003) that conventional interpretations (without a massive black hole) can match the observations equally well. Hence there is no firm empirical basis to conclude that most globular clusters harbor an intermediate mass black hole.

Nevertheless, there are plausible theoretical arguments as to why such objects should exist in at least a fraction of globular clusters (Miller & Hamilton 2002; Zheng 2001). For example, a strong correlation has been noted (Gebhardt et al. 2000; Ferrarese & Merritt 2000) between core black-hole masses and the dispersion velocity in the central bulge of the galaxies. Observed black-hole masses scale (Tremaine et al. 2002) as,

$$M_{BH} = M_0 \left(\frac{\sigma}{\sigma_0} \right)^\alpha M_\odot, \quad (14)$$

where $\alpha = 4.02 \pm 0.32$ and $M_0 \approx 1.35 \times 10^8$ for $\sigma_0 = 200 \text{ km s}^{-1}$. It has been shown (Adams et al. 2003) that this scaling simply follows because collapse to the black-hole mass is halted once the centrifugal radius of the collapse flow exceeds the capture radius of the central black hole. A similar collapse should account for formation of any spherical stellar system. Hence, it is reasonable to extrapolate this relation to globular clusters. For the 22 Milky-Way globular clusters considered in (Zheng 2001) $\sim 10\%$ would have implied black hole masses of the order of $10^3 M_\odot$, but with a large uncertainty since a long extrapolation is required. This fraction is also consistent with the fraction inferred (Miller & Hamilton 2002) from the observed luminous point sources in several starburst galaxies.

Assuming that massive black holes exist in at least some GCs, the rate at which white dwarfs pass suf-

ficiently close to a massive black hole to produce observable supernovae out to cosmological distances is given by a combination of factors,

$$\dot{N}_{MBHNS} = N_{gal} \times N_{GC} \times f_{BH} \times \lambda_{WD} \quad , \quad (15)$$

where N_{gal} is the number of galaxies out to $z \approx 1$, N_{GC} is the average number of globular clusters per galaxy, and f_{BH} is the fraction of those clusters which contain a black hole with $m_{BH} \geq 1000 M_{\odot}$.

For globular-cluster black holes, the rate λ_{WD} at which white dwarfs pass sufficiently close to explode can be written,

$$\lambda_{WD} = n_{core} \langle \sigma v \rangle \quad , \quad (16)$$

where n_{core} is the density of carbon-oxygen white dwarfs around the black hole. The quantity $\langle \sigma v \rangle$ is the average white-dwarf gravitational cross section times the virial velocity distribution in the dense environment near the black hole. Equation (16) assumes an isotropic distribution of stars and a relaxation time for the system \lesssim the rate of black-hole encounters.

The gravitational cross section σ can be written in terms of a maximum asymptotic impact parameter b ,

$$\sigma = \pi b^2 \quad , \quad (17)$$

such that a white dwarf passes close enough to the black hole for its density to exceed the pycnonuclear ignition threshold.

First, let us estimate the cross section σ . A white dwarf infalling from a large distance will have a specific angular momentum:

$$\tilde{L} = \tilde{E} v_{\infty} b \quad , \quad (18)$$

where v_{∞} is the tangential velocity component of the white dwarf at a large distance from the black hole. The specific mass-energy is given by $\tilde{E} \approx 1.0 + v_{\infty}^2/2$. This gives

$$\tilde{L} = \tilde{E} b \sqrt{2(\tilde{E} - 1)} \quad . \quad (19)$$

Now, at closest approach z_{min} ,

$$\tilde{E} = \sqrt{(1 - 2M/z_{min})(1 + \tilde{L}^2/z_{min}^2)} \quad , \quad (20)$$

which can be solved for the impact parameter b to give:

$$b^2 = \frac{2M z_{min}}{v_{\infty}^2 (1 - 2M/z_{min})} \quad . \quad (21)$$

Now inserting, $U \approx \dot{\theta} z_{min} = \tilde{L}/z_{min}$, leads to

$$U^2 \approx b^2 v_{\infty}^2 / z_{min}^2 = \frac{2M}{z_{min}(1 - 2M/z_{min})} \quad . \quad (22)$$

For the cases of interest in Tables 2 and 3, M/z_{min} is small at the distance at which the ignition density is reached and can be ignored. Solving this for b^2 and substituting $U^2 \approx 2M/z_{min}$, gives the desired cross section as a function of v_{∞} for the white dwarf, M for the black hole, and the U^2 at which the star can explode,

$$\sigma = \pi b^2 = \frac{4\pi M^2}{v_{\infty}^2 U^2} \quad . \quad (23)$$

Equivalently, one can write the cross section in terms of the distance of closest approach,

$$\sigma = \frac{2\pi M z_{min}}{v_{\infty}^2} = \pi z_{min}^2 \left(\frac{U^2}{v_{\infty}^2} \right) \quad (24)$$

Let us consider a typical globular cluster (Binney & Tremaine 1987) with a core radius of 1.5 pc, a core density of $n_{core} \approx 8 \times 10^3 M_{\odot} \text{ pc}^3$, and a core virial velocity of $v_{\infty} \approx 7 \text{ km s}^{-1}$. Even at high redshift, the core is likely to be dominated by white dwarfs with a mass distribution peaked around 0.6 M_{\odot} but with a broad distribution extending up to 1.2 M_{\odot} (Silvestri et al. 2001). We have determined the rate at which supernovae of this type are ignited per globular cluster by integrating Eq. (16) over a thermal distribution of white dwarf velocities normalized to a virial velocity of $v_{\infty} \approx 7 \text{ km s}^{-1}$. The velocity dependent gravitational cross section was taken from Eq. (24) with an average for z_{min} taken from the results of Table 2 weighted by the mass distribution of Silvestri et al. (2001). We determine in this way a rate of $\lambda_{WD} = 2 \times 10^{-8}$ SNe per year per massive black hole in a globular cluster. Hence, the use of Eq. (16) is justified since our estimated black-hole encounter rate is less than the median core relaxation time derived for GCs in the Milky Way (Binney & Tremaine 1987).

The number of galaxies out to a redshift $z \approx 1$ can be obtained by integrating the galaxy luminosity function and is approximately $N_{gal} \approx 10^9$. The number of globular clusters per galaxy is a strong function of the parent galaxy luminosity (Vandenbergh 1997). For example, in *M87* there are 1.4×10^4 globular clusters while the Milky Way only contains about 150. Since globular clusters are destroyed over time, it is quite possible the the low number of GCs in the Milky Way is atypical. If we take the number of GCs around

M87 as more realistic, then there could be more than 10^{13} globular clusters out to a redshift of $z \approx 1$.

As of yet there are no confirmed globular clusters which contain a massive black hole in the Milky Way. Nevertheless, as argued above it is at least possible that a fraction of GC's contain an as yet undiscovered massive black hole. Therefore, we allow for the possibility that $f_{BH} > 0$. The whole sky rate for this class of supernova then becomes

$$\dot{N}_{MBHSN} \approx 10^5 \frac{N_{gal}}{10^9} \frac{N_{GC}}{10^4} f_{BH} \text{ yr}^{-1} . \quad (25)$$

Although this estimate (like that for LMBHNSs) is smaller than the observed ($\sim 10^7 \text{ yr}^{-1}$) Type Ia supernova rate out to large redshift, it could be much greater if for example, the average number of globular clusters per galaxy were larger in the past. Hence, even for $f_{BH} \lesssim 0.1$, we conclude that this class of supernova event may be detectable.

5.2. Supermassive Black Holes in Galactic Centers

We next estimate the rate for the explosion of white dwarfs on passing orbits near supermassive black holes in a galactic centers. Such systems may be natural candidates for the events described here. For one, it appears that almost any moderate size galaxy has a supermassive black hole at its core (Kormendy & Richstone 1995; Magorrian et al. 1998) with a mass ranging from 10^6 to $10^9 M_\odot$ (Gebhardt et al. 2003). Furthermore, it is well know that quasars and AGN's are absorbing of order 1 to $10 M_\odot$ of material per year, and that there is a very high stellar concentration around the central supermassive black hole. For example the modest $3 \times 10^6 M_\odot$ SgrA* black hole in the Milky Way has an observed mass concentration after subtracting the black hole (Ghez et al. 1998; Genzel et al. 2003) of $1.2 \times 10^6 \times (R/10'') M_\odot \text{ pc}^{-3}$ where R is the angular distance from SgrA* in arcseconds ($1 \text{ pc} \approx 24''$ in the Galactic center). In the inner cusp, the density can exceed $10^8 M_\odot \text{ pc}^{-3}$. Although many of these stars appear to be members of a young stellar population (Figer 2000; Gezari et al. 2002), it seems likely that these young stars are the result of mergers from older stars (Schödel et al. 2003). Hence, a comparable population of white dwarfs could be present. We conservatively estimate $n_{wd} \sim 10^6 \text{ pc}^{-3}$ around the black hole with an average velocity dispersion of $v_\infty \approx 100 \text{ km s}^{-1}$.

In the case of a galactic center, equation (16) cannot be used to estimate the steady state rate at which stars fall into the BH. This is because stars on eccentric orbits that bring them close enough to the BH to be destroyed ("loss-cone" orbits) are depleted rapidly on a dynamical time scale. Subsequently, the rate is set by the much slower diffusion time-scale of stars from BH-avoiding orbits into radial orbits. Here we will apply the loss cone model as discussed in Syer & Ulmer (1999) and Magorrian & Tremaine (1999).

In this model the two-body relaxation timescale for a spherical cluster of stars of mass m_* with a density $\rho(r)$ and an isotropic density dispersion $\sigma(r)$ is given by,

$$t_r = \frac{\sigma^3}{\ln \Lambda G^2 \rho m_*}, \quad (26)$$

where m_* is the typical stellar mass and Λ includes dimensionless factors of order unity as well as the Coulomb logarithm. Following Binney & Tremaine (1987) and Syer & Ulmer (1999) we then can write a numerical value of:

$$t_r = \frac{1.8 \times 10^{10} \text{ y}}{\ln(0.4 \times N)} \left(\frac{\sigma}{100 \text{ km s}^{-1}} \right)^3 \times \left(\frac{M_\odot}{m_*} \right) \left(\frac{10^4 M_\odot \text{ pc}^{-3}}{\rho} \right), \quad (27)$$

where N is the number of stars within the characteristic radius r_b and σ is the one-dimensional velocity dispersion (Seyfer & Ulmer 1999) given as

$$\sigma^2 \approx \frac{GM}{(1+p)r}, \quad (28)$$

where $p \sim 2$ is the logarithmic slope of the density. The white dwarf capture rate will then be given by the rate at which white dwarfs will scatter into the loss cone.

$$\lambda_{WD} \approx \int \frac{4\pi n_{wd}(r) r^2 dr}{\ln(2/\theta_{lc}) t_r}, \quad (29)$$

where $n_{wd}(r)$ is the number density of white dwarfs

$$n_{wd} = f_{wd} \rho / \langle m_{wd} \rangle, \quad (30)$$

where $f_{wd} \sim 0.5$ is the mass fraction in white dwarfs and $\langle m_{wd} \rangle \sim 0.6 M_\odot$ is the mean white-dwarf mass. The quantity $\theta_{lc} = qGM/r^2 \sigma^2$ is the angular size of the "loss cone" where q is the radius at which stars are removed from the system. The density profile $\rho(r)$ divides into inner and outer regions. The black hole

dominates the gravity in the inner region so that a density profile of the form $\rho \approx r^{-2}$ and a dispersion velocity, $\sigma^2 \approx GM/3r$ is expected. In the outer region on the other hand one expects flatter density and velocity-dispersion contours. Based upon the analysis of Syer & Ulmer (1999) (cf. their figure 4) we estimate $\lambda_{WD} \sim 3 \times 10^{-5}$ for a typical white dwarf mass of $0.6 M_{\odot}$. However, based upon the range and uncertainties in the parameters ρ , σ , r_b , and M_{BH} we expect a range in λ_{WD} from up to an order of magnitude above to a couple of orders of magnitude below this number. For purposes of discussion we will adopt $\sim 3 \times 10^{-5}$ as a reasonable estimate.

The total rate of such events out to $z \approx 1$ will be given by a similar combination of the factors to those given above in Eq. (15),

$$\dot{R}_{SMBHSN} = N_{gal} N_{SM} \lambda_{WD} , \quad (31)$$

where again, $N_{gal} \sim 10^9$ is the number of galaxies out to $z \approx 1$ and $N_{SM} \sim 1$ is the number of supermassive black holes per galaxy. The quantity λ_{WD} is again the rate at which white dwarfs are making sufficiently close passes to a black hole. The total rate is then of order 10^3 to a few $\times 10^5 \text{ yr}^{-1}$. This rate is somewhat less than normal SN1a's which are observed at a rate $\sim 10^7 \text{ yr}^{-1}$. Furthermore, a large fraction of such events might be hidden in the dense regions surrounding galactic cores. Nevertheless, this crude estimate is at least suggestive that such events could be frequent enough to be observed. It is conceivable that they might even dominate over normal Type Ia supernovae at sufficiently large redshift where newly formed galactic cores have not yet depleted their radial orbits. Frequent white dwarf encounters with a supermassive black hole might even provide a power source for AGNs and quasars. Clearly, if such explosions occur, a search for observed signatures seems warranted.

6. Possible Observed Signatures

Having proposed this class of new supernovae it is worth commenting on several distinguishing characteristics which might help observers identify whether one of these events has actually occurred. Preliminary numerical burn simulations (D. Dearborn, priv. comm.) of $0.6 M_{\odot}$ white dwarfs passing a supermassive black hole indicate a nearly complete burn of initial C/O into Ni/Co. Hence, each supernova should indeed generate $\sim 10^{51}$ erg in kinetic energy of mat-

ter and $\sim 10^{49}$ erg in optical light. The optical signal, however, may be unique for several reasons.

One obvious feature is that these supernovae should most likely be seen in association with a galactic core (or possibly a globular cluster). Indeed, a number of transients that might be such supernovae near galactic cores have been observed (N. Suntzeff, priv. comm.) out to large redshift, but are often not analyzed due to the complication of their location in a crowded field. We suggest that in the near future, the development of the National Virtual Observatory (cf. Hanisch 2002) might be utilized to search for a possible association of unusual Type I supernovae with galactic cores and/or extragalactic globular clusters.

Among other things to look for is the fact that the stars are moving very fast when they explode. Hence, they could exhibit a large Doppler shift in their spectra. Also, the explosion itself should be different, since the stars are of lighter mass and undergo a very rapid rapid compression/ignition. Normal Type Ia events are expected to undergo an off-center ignition after a gradual approach to the ignition density. The events described here, however, will probably ignite rapidly and at their centers. This will cause a detonation and a possibly more efficient thermonuclear burn of the white dwarf (depending upon tidal effects from the black hole). Thus, one might expect a different burn front, a different light curve, and different nucleosynthesis yields (e.g. more iron and reduced silicon) compared to normal SNIa events.

6.1. Interaction with the Black Hole

Another distinguishing characteristic of these explosions is that they occur in the strong field of a companion black hole. Hence, there might be an affect on the light curve from matter accreting into the black hole and/or impinging on the accretion disk. For example, the accretion of SN debris onto the black hole might produce excess X-ray (or even γ -ray) emission.

We suggest two possible observational consequences of the SMBHSNe, depending upon the optical depth of the material in the accretion disk down to the location where the supernova occurs. If the optical depth to the point of explosion is greater than one, then since the scale of the systems is so large, energy will be emitted from the system over a timescale of a year or more.

In the case that the optical depth is less than one then the usual SN light signal will be seen. However,

if there is an accretion disk present, then the SN light signal will be augmented by radiation emitted from the collision of the SN remnant with the accretion disk.

Let us consider order-of-magnitude estimates for the radiation emitted as debris from the explosion of a $0.6 M_{\odot}$ white dwarf impinges on the accretion disk of a 10^9 solar mass black hole. For this we will assume that the accretion disk is flat. That is, we ignore the thickness of the accretion disk near the black hole.

From Table 3, the distance from the black hole to the point at which the explosion initiates is typically about $d = 1.5 \times 10^{15}$ cm (roughly ten black hole Schwarzschild radii). We take this as a measure of the distance from the supernova to the accretion disk. The expansion velocity of the supernova shell is given by $v \approx (2 \times 10^{51}/M_{WD})^{1/2} = 1.3 \times 10^9$ cm s^{-1} . Hence, the time scale for material to reach the accretion disk is of the order $1.5 \times 10^{15}/v \approx 10^6$ sec. The time for peak luminosity of a Type-I supernova is also about 10^6 sec. Thus, the peak supernova signal and the start of the thermal radiation from the collision of the supernova remnant with the accretion disk will typically occur at about the same time.

The peak temperature from the collision shock will be about 400 keV. The electrons and baryons will come to equilibrium temperatures quickly. Then bremsstrahlung radiation will cool the hot gas on a timescale of about 10^4 sec. Most of the remnant will not hit the accretion disk perpendicularly. Averaging the various physical quantities over the angle of impact we estimate a mean photon energy of about 30 keV. The time for the photon spectrum to fall below 10 keV will be about 10^7 sec. The total emitted X-ray energy will be $\sim 10^{50}$ ergs. Thus, an X-ray burst in coincidence with a supernova explosion deep inside a galaxy is what we expect to possibly be observed.

6.2. Remnants

As another observed signature, it is possible that remnants from this type of supernova may be detectable in the Galaxy. For example, an event rate of a few $\times 10^{-5}$ y^{-1} per galaxy for white dwarfs to approach and explode near the giant black hole in galaxy centers, suggests that it is worthwhile to search for a supernova remnant with an age $\approx 3 \times 10^4$ y near the giant black hole SgrA* in the Galactic center. For a remnant moving with a typical dispersion velocity of 100 km s^{-1} for 10^4 y, one would expect to find such

a remnant ~ 1 pc from SgrA*.

In this regard, it is certainly of interest that indeed such a remnant (SgrA East) exists and has been recently analyzed (Maeda et al. 2002) with the ACIS detector aboard the *Chandra X-ray Observatory*. This remnant is centered at a distance of ≈ 3 pc from SgrA*. In fact, SgrA* is within the remnant outer rim. The passage of the supernova shell sometime in the past may have swept gas away from the black-hole vicinity and hence, may be responsible for the present quiescent state of SgrA*. Also of note is the fact that its peculiar metal abundances, along with the unusual combined radio and X-ray morphologies classifies this remnant as a metal-rich "mixed-morphology" (MM) SNR. Although, the properties of SgrA East may be explained (Maeda et al. 2001) by a low-mass Type II supernova, it is tempting here to speculate that this class of MM SNRs may be the smoking gun for a black-hole induced white-dwarf explosion (cf. Khokhlov & Melia 1996).

Obviously, a clear picture of how to classify these events will require fully relativistic numerical computations in three spatial dimensions of the compression and thermonuclear explosion of a white dwarf in the background field of a black hole. Efforts along this line are currently under way (D. Dearborn priv. comm.) utilizing three dimensional hydrodynamics and radiation transport. As noted above, preliminary results indicate a central thermonuclear ignition (very close to our adopted ignition density) which proceeds to detonate the star. In future work we will simulate the radiation transport, light curve, and supernova remnant.

7. Conclusions

We have explored a new class of Type-I supernovae whereby the onset of a thermonuclear explosion is induced by relativistic enhancements of the white-dwarf self gravity as it accelerates in the background gravitational field of a black hole. We find that a potentially observable rate of such events could be occurring out to cosmological distances, particularly in the dense regions of galactic cores and possibly globular clusters as well. These explosions and their remnants could thus be characterized by their association with supermassive black holes galactic cores or massive black holes in globular clusters. They also might be characterized by an associated x-ray burst and/or

a significantly modified light curve from matter colliding with the black-hole accretion disk.

Work at the Lawrence Livermore National Laboratory performed in part under the auspices of the U. S. Department of Energy under contract W-7405-ENG-48 and NSF grant PHY-9401636. Work at the University of Notre Dame supported by the US Department of Energy under Nuclear Theory grant DE-FG02-95ER40934.

REFERENCES

- Adams, F. C., Graff, D. S., Mboyme, M. & Richstone, D. E. 2003, ApJ, 591, 125
- Arnowitt, R., Deser, S. & Misner, C. W. 1962, in *Gravitation*, ed. L. Witten (New York: Wiley), p. 227
- Ayal, S., Livio, M. & Piran, T. 2000, ApJ, 545, 772
- Baumgardt, H., Makino, J., Hut, P., McMillan, S., Portegies Zwart, S. 2003, ApJ, 589, L25.
- Binney, J. & Tremaine, S. 1987, in *Galactic Dynamics*, (Princeton University Press: Princeton).
- Carter, B. & Luminet, J. P. 1982, Nature, 296, 377
- Cowley, A. P. 1992, ARA&A, 30, 287
- Ferrarese, L. & Merritt, D. 2000, ApJ, 539, L9
- Ferraro, F. R., Possenti, A., Sabbi, E., Lagani, P., Rood, R. T., D'Amico, N., Origlia, L. 2003, AJ, 595 179
- Figer, D. F., et al. 2000, ApJ, 533, L49
- Freedman, W. L., et al. 2001, ApJ, 553, 47
- Freudling, W., Corbin, M. R., & Korista, K. T. 2003, ApJ, 587, 67
- Fryer, C. L., Herant, M. & Davies, M. V. 1999, ApJ, 520, 650
- Gebhardt, O., Kronawitter, A., Sagalia, R. P. & Bender, R. 2001, AJ, 121, 1936
- Gebhardt, K., et al. 2000, ApJ, 539, L13
- Gebhardt, K., Rich, R. M. & Ho, L. C. 2002, ApJ, 578, 41
- Gebhardt, K., et al. 2003, ApJ, 583, 92.
- Genzel, R. et al. 2003a, ApJ, 594, 812
- Schödel, R. et al. 2003, ApJ, 596, 1015
- Gerssen, J., van der Marel, R. P., Gebhardt, K., Guhathakurta, P., Peterson, R. C., & Pryor, C. 2002, AJ, 124, 3270
- Gezari, S. et al. 2002 ApJ, 520, 650
- Ghez, A. M., Klein, B. L., Morris, M. & Becklin, E. E. 1998, ApJ, 509, 678
- Garnavich, P. M. et al. 1998, ApJ, 509, 74
- Greggio, L. & Renzini, A. 1983, A&A, 118, 217
- Hamada, T. & Salpeter, E. E. 1961, ApJ 134, 683
- Hanisch, R. J. 2002, in *Virtual Observatories*, Edited by Szalay, Alexander S. Proceedings of the SPIE, Volume 4846, pp. 13-19
- J. Hawley, L. Smarr & J. R. Wilson, *Astrophys. J. Suppl.*, **55**, 211 (1984).
- Iben, I. Jr. & Tutukov, A. V. 1984, ApJS, 54, 355
- Iben, I. Jr. & Tutukov, A. V. 1985, ApJS, 58, 661
- Iwamoto, K. et al. 1999, ApJS, 125, 439
- Khokhlov, A. & Melia, F. 1996, ApJ, 457, L61
- Kobayashi, C., Tsujimoto, T. & Nomoto, K. 2000, ApJ, 539, 26
- Kormendy, J. & Richstone, D. 1995, ARA&A, 33, 581
- Kraicheva, Z. T., Popova, E. I., Tutukov, A. V., & Yungelson, L. R. 1979, *Soviet Astro.*, 23, 29
- Laguna, P., Miller, W. A. & Zurek, W. H. 1994, *Mem. S. A. It.*, 65, 1129
- McNamara, B. J., Harrison, T. E. & Anderson, J. 2003, ApJ, 595, 187
- Maeda, Y. et al., 2002, ApJ, 570, 671
- Magorrian, J., et al., 1998, AJ, 115, 2285
- Magorrian, J. & Tremaine, S., 1999, MNRAS, 309, 447)
- Mathews, G. J., Bazan, G. & Cowan, J. J. 1992, ApJ, 391, 719

Mathews, G. J., Marronetti, P. & Wilson, J. R. 1998, PRD58, 043003

Mathews, G. J. and Wilson, J. R. 2000, Phys. Rev. D 61, 127304

Miller, M. C. & Hamilton, D. P. 2002, MNRAS, 330, 232

Nomoto, K., et al. 1994, in *Cosmic Explosions*, ed. S. S. Holt & W. W. Zhang (New York: AIP), p. 35

Perlmutter, S. et al. 1998, Nature **391**, 51 (1998); Astrophys. J., **517**, 565 (1998).

Provencal, J. L., Shipman, H. L., Hog, E., & Thejll, P. 1998, ApJ 494, 759

Rathore, Y., Broderick & Blanford, R.D. 2003, MNRAS, 339, 25; 2000, BAAS, 197, 118.08

Riess, A. et al., 1998, AJ, 116, 1009

Salpeter, E. E. 1961, ApJ 134, 669

Silvestri, N. M. et al. 2001, ApJ, 121, 503

Syer, D. & Ulmer, A. 1999, MNRAS, 306, 35

Tremaine, S. et al. 2002, ApJ, 574, 740

Tutukov, A. V. & Yungelson, L. R. 1979, Acta. Astron., 23, 665

van der Marel, R. P., Gerssen, J., Guhathakurta, P., Peterson, R. C., & Gebhardt, K. 2002, AJ, 124, 3255

Wilson, J. R. 1979, in *Sources of Gravitational Radiation*, ed. L. Smarr (Cambridge; Cambridge Univ. Press) p. 423.

Wilson, J. R. 2000, PRD, 66, 084015

Wilson, J. R. & Mathews, G. J., 2003, *Relativistic Numerical Hydrodynamics*, (Cambridge University Press, Cambridge), in press

Wilson, J. R., Mathews, G. J. & Marronetti, P. 1996, Phys. Rev. D54, 1317

Zheng, X.-Z., Chin. J. A&A, 1, 291

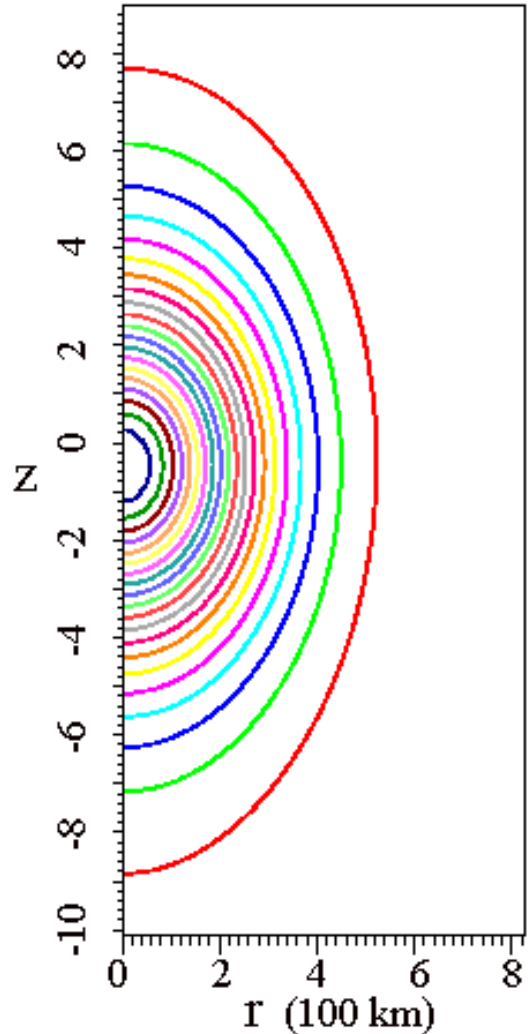


Fig. 1.— Contours of constant density in the r vs. z plane for a $0.6 M_{\odot}$ white dwarf approaching a $1000 M_{\odot}$ black hole. The star is near closest approach, centered at $z \approx 1.4 \times 10^4$ km from the black hole which is located below the figure. This star is tidally distorted to an aspect ratio of $(z, r) \approx (900, 500)$ km. Nevertheless, the radius has contracted by a factor of 10 from that of an isolated star. The central density has correspondingly increased by more than a factor of 1000 from (3.2×10^6) to $(3.3 \times 10^9 \text{ g cm}^{-3})$ which is above the pycnonuclear ignition threshold.

This 2-column preprint was prepared with the AAS L^AT_EX macros v4.0.

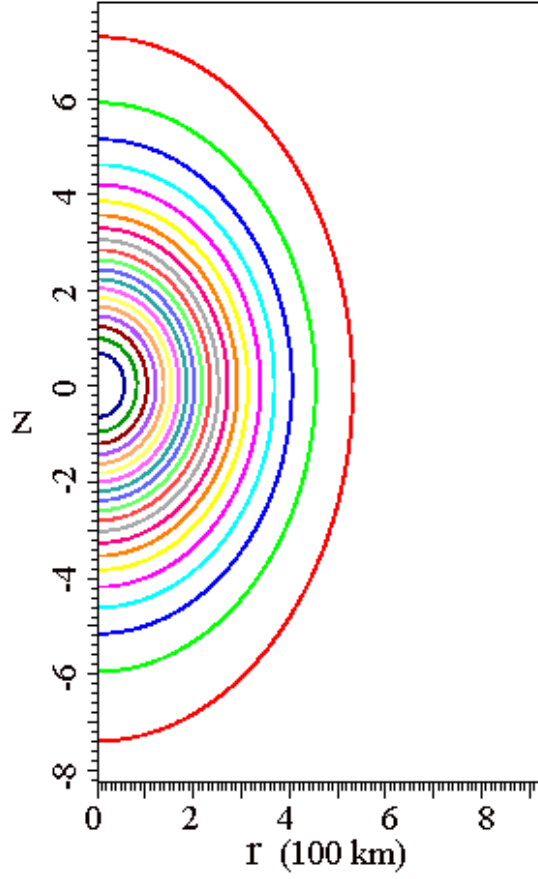


Fig. 2.— Contours of constant density in the r vs. z plane for a $0.6 M_{\odot}$ white dwarf near closest approach ($z \approx 2 \times 10^4$ km) to a $1500 M_{\odot}$ black hole.

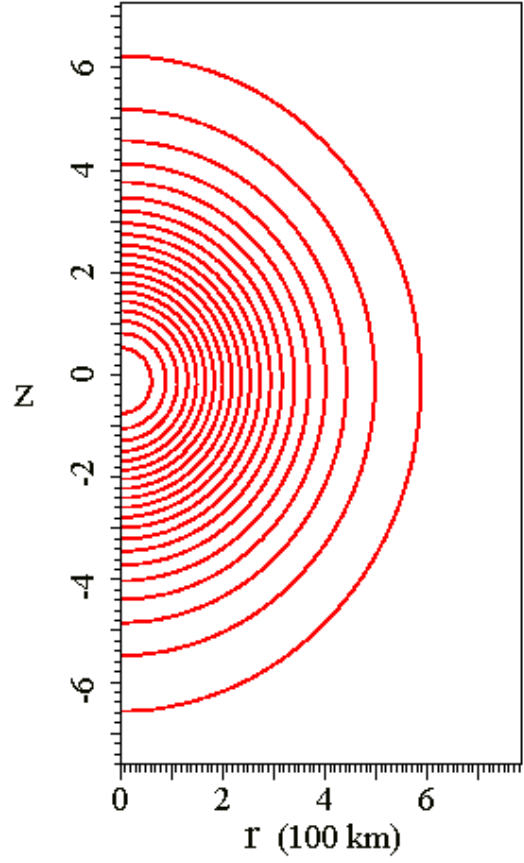


Fig. 3.— Contours of constant density in the r vs. z plane for a $0.6 M_{\odot}$ white dwarf near closest approach ($z \approx 4 \times 10^4$ km) to a $3000 M_{\odot}$ black hole.